Journal of Membrane Science 549 (2018) 377–384

Contents lists available at ScienceDirect

Journal of Membrane Science

journal homepage: www.elsevier.com/locate/memsci

Mixed-matrix membranes containing an azine-linked covalent organic framework: Influence of the polymeric matrix on post-combustion CO_2-capture

Meixia Shan[a], Beatriz Seoane[b,*], Eduardo Andres-Garcia[a], Freek Kapteijn[a], Jorge Gascon[a,c,**]

[a] Catalysis Engineering, Chemical Engineering Department, Delft University of Technology, van der Maasweg, 9, 2629 HZ Delft, The Netherlands
[b] Faculty of Science, Debye Institute for Nanomaterials Science, Utrecht University, Universiteitsweg 99, Utrecht 3584 CG, The Netherlands
[c] King Abdullah University of Science and Technology, KAUST Catalysis Center, Advanced Catalytic Materials, Thuwal 23955, Saudi Arabia

ARTICLE INFO

Keywords:
Covalent organic frameworks
Mixed-matrix membranes
CO_2/N_2 separation
CO_2 capture

ABSTRACT

The use of an azine-linked covalent organic framework (ACOF-1) as filler in mixed-matrix membranes (MMMs) has been studied for the separation of CO_2 from N_2. To better understand the mechanisms that govern separation in complex composites, MMMs were prepared with different loadings of ACOF-1 and three different polymers as continuous phase: low flux-mid selectivity Matrimid®, mid flux-high selectivity Polyactive™ and high flux-low selectivity 6FDA:DAM. The homogeneous distribution of ACOF-1 together with the good adhesion between the ACOF-1 particles and the polymer matrices were confirmed by scanning electron microscopy. In mixed-gas CO_2/N_2 separation a clear influence of the polymer used was observed on the performance of the composite membranes. While for Matrimid® and 6FDA:DAM an overall enhancement of the polymer's separation properties could be achieved, in case of Polyactive™ penetration of the more flexible polymer into the COF porosity resulted in a decreased membrane permeability. The best improvement was obtained for Matrimid®-based MMMs, for which a selectivity increase from 29 to 35, together with an enhancement in permeability from 9.5 to 17.7 Barrer for 16 wt% COF loading, was observed. Our results demonstrate that the combination of the filler-polymeric matrix pair chosen is crucial. For a given filler the polymer performance improvement strongly depends on the polymeric matrix selected, where a good match between the discontinuous and continuous phase, both in the terms of compatibility and gas separation properties, is necessary to optimize membrane performance.

1. Introduction

Global warming has caused great public concern due to the fast increase of emissions of greenhouse gases, especially CO_2. Capture of CO_2 from flue gas streams of fossil-fuelled power plants, which account for about 40% of the total carbon emissions worldwide, will be instrumental in addressing measures against climate change [1,2]. Flue gas is composed of different gases such as CO_2, N_2, CO, O_2, water vapour and sulfur oxide, where N_2 is the main component and the concentration of CO_2 (volume basis) is around 15% [2,3]. Thus, the separation of CO_2 from CO_2/N_2 mixtures is usually studied in the development of new separation technologies for post-combustion CO_2 capture.

Conventional technologies for gas separation, such as cryogenic distillation, condensation or amine absorption, are energy intensive and may pose environmental concerns. Membrane separation technology, on the other hand, has been greatly developed in recent years for CO_2 capture owing to its attractive features like inherent simplicity, easy operation, energy efficiency, and often smaller footprints. Among the different types of membranes [4–6] those based on polymers are the most widely used in the current market, mainly due to their good processability and low cost. However, polymeric membranes suffer from a well-known trade-off relationship between permeability and selectivity, as originally reported by Robeson in 1991 [7,8]. Moreover, their limited thermal and chemical stability and the CO_2-induced plasticization [9,10] also restrict their massive application. Better separation properties and chemical and thermal stabilities can be achieved with inorganic membranes, but they lack mechanical stability and suffer from processability and high cost issues [11]. In this sense, mixed-matrix membranes (MMMs), where selected fillers are dispersed in a continuous polymer matrix, were proposed to overcome the limitations of organic and inorganic membranes, aiming at the synthesis of

* Corresponding author.
** Corresponding author at: Catalysis Engineering, Chemical Engineering Department, Delft University of Technology, van der Maasweg, 9, 2629 HZ Delft, The Netherlands.
E-mail addresses: b.seoanedelacuesta@uu.nl (B. Seoane), jorge.gascon@kaust.edu.sa (J. Gascon).

https://doi.org/10.1016/j.memsci.2017.12.008
Received 17 August 2017; Received in revised form 26 October 2017; Accepted 4 December 2017
Available online 06 December 2017
0376-7388/

processable membranes with a performance above the Robeson trade-off limit. Many different polymers, such as different polyimides [12,13], polysulfone (PSF) [14] and polybenzimidazole (PBI) [15,16] have been used for the fabrication of MMMs, whereas zeolites [17], carbon materials [18], and metal-organic frameworks (MOFs) [19,20] are porous fillers commonly used. Among these fillers, MOFs have demonstrated great prospect in preparing MMMs for CO_2 separation due to their high porosity, selectivity towards certain guest molecules and rich pre- and post-synthetic chemistry [21]. However, most MOFs show poor stabilities in humid conditions, which limit their application in real-life CO_2 capture [22]. Despite long-term stability of MOF-based MMMs with respect to moisture is of utmost importance, this issue remains largely unexplored and thus, still needs to be addressed.

As an alternative to MOFs, covalent organic frameworks (COFs) have recently emerged as potential candidates for the preparation of MMMs. COFs are a class of crystalline porous materials constructed from light-weight elements linked by strong covalent bonds [23,24]. They have attracted tremendous interest due to their exceptional properties such as low densities, regular and permanent porosity, high surface areas and high thermal stabilities, appealing in different fields, like gas storage and separation [25], catalysis [26] and photovoltaics [27]. Different MMMs have been reported in which COFs have been used as porous fillers [28–31]. Biswal et al. [32] dispersed two different chemically stable isoreticular COFs (TpPa-1 and TpBD) in PBI-Bul, obtaining hybrid membranes with H_2, N_2, CO_2, CH_4 permeabilities up to seven times higher than those of the bare polymer at relatively unchanged CO_2/N_2 and CO_2/CH_4 separation factors. Wang and co-workers [33] prepared highly compatible MMMs containing PVAm and COF for H_2/CO_2 separation, and the resulting membranes showed a notable improved gas permeability together with slightly higher H_2/CO_2 selectivities. Zhao et al. [34] successfully incorporated two COFs (NUS-2 and NUS-3) into two different polymer matrices (Ultem® and PBI) and applied the membranes to CO_2/CH_4 and H_2/CO_2 gas separation. The NUS-2@PBI membranes showed an increase in the H_2/CO_2 selectivity from 9 for the bare polymer up to 31 upon 20 wt% COF loading, exceeding the upper bound reported by Robeson in 2008. Recently, our group reported azine-linked COF (ACOF-1)@Matrimid® MMMs for CO_2/CH_4 separation. A more than doubling of the CO_2 permeability together with slightly higher CO_2/CH_4 separation factors were observed upon 16 wt% ACOF-1 loading compared to the bare Matrimid® polymer [35]. These first examples illustrate the potential of COFs as fillers in the preparation of defect free MMMs. The fully-organic nature of COFs probably accounts for this good adhesion between dispersed and continuous phases, in contrast to other traditional porous fillers, such as zeolites, for which their inorganic nature commonly lead to the formation of defects at the filler-polymer interface. However, choosing appropriate polymer and COF pairs for specific gas mixtures is of high importance to fully exploit the COF separation properties. For a given COF, different polymers can be potentially used as the continuous polymeric matrix and vice versa, the proper combination of COF and polymer being key for the fabrication of promising MMMs for gas separation. Indeed, the importance of an appropriate selection of a polymer/filler pair has been recently highlighted by the work of Bae et al. [36] Using atomically detailed simulations and theoretical permeation models, Keskin and co-workers [37,38] predicted the separation performance of several new MMMs composed of various polymers and MOFs, and the results provided some suggestions for selecting suitable polymer/MOF pairs to obtain improved separation results. However, despite the importance of such design predictions, no similar works have been reported for the preparation of COF-based MMMs.

Herein, the influence of the polymeric matrix on the membrane performance for a given COF was studied. ACOF-1 was selected as filler since it has shown high CO_2 adsorption selectivity from N_2 in powder form together with a good stability [39]. Three different polymers with different separation properties, namely the low flux-mid selectivity Matrimid®, mid flux-high selectivity Polyactive™ and high flux-low selectivity 6FDA:DAM, were chosen as the continuous matrices. The resulting MMMs have been tested for CO_2/N_2 separation. The best results were obtained for Matrimid®-based MMMs, for which no non-idealities were observed at the filler/polymer interface and a good match between filler and polymer permeation properties allowed for the increase of the MMM permeability. Overall, our study provides some insight into the important topic of the selection of the filler/polymer pair in COF-based MMMs.

2. Experimental section

2.1. Materials

Benzene-1,3,5-tricarboxaldehyde (97%), hydrazine hydrate (N_2H_4 50–60%), 1,4-dioxane (99.8%), acetic acid, tetrahydrofuran (THF) (99.9%), and acetone (99.9%) were purchased from Sigma Aldrich. All these starting materials and solvents were used without further purification. Matrimid® 5218 (M_w = 123,000 g mol^{-1}, $M_n \approx$ 11,000 g mol^{-1}) was kindly supplied by Huntsman Advanced Materials. 6FDA: DAM polyimide (M_w = 271,876 g mol^{-1}, $M_n \approx$ 121,875 g mol^{-1}) and Polyactive™ (M_w = 35,000 g mol^{-1}) were purchased from Akron polymer systems and PolyVation, respectively. Fig. 1 shows the chemical structure of the different polymers used. All the polymers were dried prior to use to remove the adsorbed moisture under vacuum conditions for 48 h at 453 K, 433 K and 323 K for Matrimid®, 6FDA:DAM and Polyactive™, respectively.

2.2. Synthesis of ACOF-1

ACOF-1 was synthesized following the same procedure as described in the previous work [35,39]. In a typical synthesis, a 10 mL Pyrex tube 1 was charged with 1,3,5-triformylbenzene (60 mg, 0.37 mmol), dioxane (2.0 mL) and acetic acid (AcOH, 0.2 mL, 6 M). Another 10 mL Pyrex tube 2 was charged with hydrazine hydrate. Both tubes were degassed under Ar for 1 h and then 32 μL hydrazine hydrate was transferred from tube 2 to tube 1. Afterwards, tube 1 was tightly covered and the mixture was sonicated for 2 min and heated at 393 K for 72 h. The resulting powder was centrifuged at 5000 rpm for 10 min, washed thoroughly with anhydrous dioxane, anhydrous tetrahydrofuran and anhydrous acetone and finally dried under vacuum at 373 K overnight to give a pale-yellow powder (42 mg).

2.3. Preparation of mixed-matrix membranes (MMMs)

For Matrimid® and 6FDA:DAM MMMs fabrication, the required amount of ACOF-1 particles was first dispersed in THF and sonicated for 30 min. To this suspension, 0.2 g dried polymer were added and the casting suspension was further stirred for 24 h. The solvent/filler-polymer weight ratio was kept at 90/10 in all cases. The proportion of ACOF-1 in the casting suspension was adjusted to achieve the desired final ACOF-1 loadings of 8 wt% and 16 wt% in the resulting MMMs.

The prepared suspensions were then cast onto a clean glass plate with the help of a doctor blade knife. The cast membranes were then immediately covered with a small watch glass to prevent a too fast evaporation of the solvent. The glass plate was further covered with a square box with four small bottles of THF inside to create a saturated THF atmosphere. All these measures were taken to slow down the evaporation rate of THF and thereby preventing the formation of defects during drying. The membrane was first left to dry overnight at room temperature and then dried under vacuum for 24 h (423 K for Matrimid®-based and 433 K for 6FDA:DAM-based membranes).

For Polyactive™ MMMs preparation, the ACOF-1 particles were dispersed in THF and sonicated for 30 min. To this suspension, 0.2 g Polyactive™ was added and the casting suspension was further stirred for 24 h. Afterwards, the prepared solution was poured into a Teflon petri dish, which was covered with a square box with four small bottles

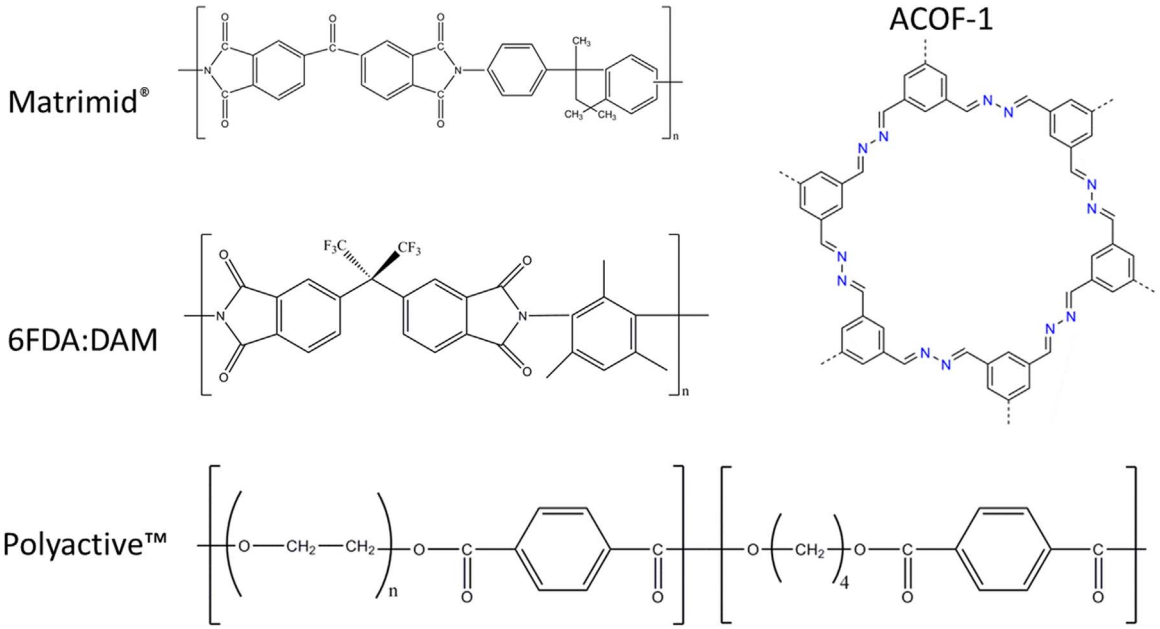

Fig. 1. Chemical structure of the polymers used together with that of ACOF-1 used as porous filler.

of THF inside to create a saturated THF atmosphere. The membrane was first left to dry overnight and then dried under vacuum at 323 K for 24 h.

For the three polymers, the pure polymer membranes were prepared following the same procedure as for the MMMs, but without the extra step of dispersing ACOF-1 particles. The final thickness of the resulting membranes was individually evaluated using a digital micrometer.

2.4. ACOF-1 and membrane characterization

Diffuse reflectance infrared Fourier transform (DRIFT) spectra of ACOF-1 powder was acquired in a Nicolet 8700 FT-IR (Thermo Scientific) spectrometer equipped with a high temperature cell with CaF_2 windows. The samples were pretreated in a He flow at 393 K for 5 min prior to collecting the spectra.

Raman measurements were performed on the ACOF-1 powders with a Jobin Yvon Labram 300 confocal microscope equipped with a laser at 633 nm and a 1800 lines/mm grating.

The solid-state ^{13}C cross-polarization magic-angle spinning (CP/MAS) NMR spectra were acquired at ambient temperature by a Bruker Advance 400 solid-state NMR spectrometer at a spinning rate of 10 kHz. The chemical shift of dilute tetramethylsilane (TMS) in $CDCl_3$ (external) was used as reference. The operating frequency is 100.6 MHz.

Powder X-ray diffraction (PXRD) patterns of the prepared membranes were recorded using a Bruker-D8 Advanced diffractometer with Co-K_α radiation (λ = 1.78897 Å). The samples were scanned in the 2θ range of 5–80° using a step size of 0.02° and a scan speed of 0.4 s per step in a continuous scanning mode.

Scanning electron microscopy (SEM) micrographs were acquired using a JEOL JSM-6010LA InTouchScope microscope equipped with an integrated SDD EDS detector. ACOF-1 specimens were prepared by drop-casting a sonicated methanol ACOF-1 suspension directly on the sample holder followed by gold sputtering for 20 s. Cross-section of the membranes were obtained by cryo-fracturing in liquid nitrogen.

N_2-physisorption was carried out at 77 K in a Quantachrome Autosorb-6B setup. CO_2 adsorption isotherms of ACOF-1 and membranes were recorded in a Tristar II 3020 (Micromeritics) at 273 K. Prior to the gas adsorption measurements, the samples were degassed at 393 K under N_2 flow for at least 16 h.

CO_2 and N_2 high-pressure adsorption experiments were measured at 273 K, 298 K and 308 K with a volumetric apparatus from BEL Japan (Belsorp-HP). In all cases, around 0.1 g sample was outgassed overnight under vacuum conditions at 393 K.

Thermogravimetric analysis (TGA) was performed on a Mettler Toledo TGA/SDTA851e apparatus by measuring the mass loss of the sample while heating ACOF-1 and the prepared membranes under N_2 (100 mL min^{-1}) from room temperature to 1073 K at a heating rate of 10 K min^{-1}.

Differential scanning calorimetry (DSC) measurements were carried out using a Perkin Elmer DSC 7 to assess the glass transition temperature (T_g) of the neat membrane and MMMs. The scanning range was 298–698 K at a heating rate of 10 K/min under N_2 atmosphere for 6FDA:DAM and Matrimid®-based membranes and 198–348 K for Polyactive™ membranes. Two consecutive runs were performed. A first DSC cycle was performed to remove thermal history and adsorbed water from the samples. After cooling, a second cycle was performed following the same procedure. The glass transition temperature (T_g) value was determined as the point in the transition region where the step change in heat capacity (C_p) attains half the value of the total step in the DSC curve [40].

2.5. Gas permeation experiments

Membrane areas of 3.14 cm^2 were cut from the casted membrane films, placed on a macroporous support and mounted in a flange between Viton® O-rings. This flange fits in a permeation module, which was placed inside an oven in a permeation home-made setup described elsewhere [14]. The CO_2/N_2 separation measurements were performed employing a 15:85 CO_2:N_2 gas mixture (23 mL min^{-1} CO_2 and 130 mL min^{-1} of N_2) as feed. Helium (4.6 mL min^{-1}) was used as sweep gas at the permeate side. The absolute pressure of the feed stream was adjusted in a range of 2–5 bar using a back-pressure controller at the retentate side, keeping the permeate side at atmospheric pressure. The temperature in the permeation module was kept at 308 K. An on-line gas chromatograph (Interscience Compact GC) equipped with a packed Carboxen 1010 PLOT (30 m × 0.32 mm) column and TCD detector was used to periodically analyze the permeate stream. Each membrane was fabricated and measured at least 3 times to ensure reproducibility of the reported data. In all cases, gas separation performance was evaluated after ensuring steady state operation.

Gas separation performance was defined by the separation factor (α) and the gas permeability (P) of the individual components. The

permeability for component i (P_i) was calculated as follows (Eq. (1)):

$$P_i = \frac{F_i \cdot l}{\Delta p_i \cdot A} \quad (1)$$

where flux F_i denotes the molar flow rate of compound i, l is the thickness of the membrane and A is the membrane area. Δp_i is the partial pressure difference of component i across the membrane and it can be calculated according to Eq. (2).

$$\Delta p_i = p_{feed} \times Y_{i,\ feed} - p_{perm} \times X_{i,\ permeate} \quad (2)$$

where p_{feed} *and* $p_{permeate}$ represent the pressures at the feed and permeate sides and $Y_{i,\ feed}$ and $X_{i,\ permeate}$ are the molar fractions of the component i in the feed and permeate gas streams, respectively. The thickness of the membrane was measured by a digital micrometer (Mitutoyo, IP54 Absolute Digimatic Micrometer, MDQ-30, range 0–30 mm, accuracy ± 0.001 mm). The average thickness were calculated from 10 different measurements at different spots of the membrane.

The SI unit for the permeability is mol s^{-1} m^{-1} Pa^{-1}. However, gas permeabilities are reported in the widely used non-SI unit Barrer, where 1 Barrer = 3.35 × 10^{-16} mol s^{-1} m^{-1} Pa^{-1}.

The separation factor or mixed gas selectivity (α) was calculated as the ratio of the permeability of the more permeable compound (CO_2), to the permeability of the less permeable compound (N_2) (Eq. (3)).

$$\alpha = \frac{P_{CO2}}{P_{N2}} \quad (3)$$

3. Results and discussion

3.1. Characterization of ACOF-1

The synthesis of ACOF-1 particles was performed following the method as previously described [35,39]. ACOF-1 particles were characterized by means of DRIFT, Raman and solid-state ^{13}C cross-polarization magic-angle spinning (CP/MAS) NMR spectroscopy together with XRD and N_2 and CO_2 adsorption. The formation of the C = N bond upon ACOF-1 synthesis was confirmed by the acquired DRIFT, Raman and NMR spectra. Particularly, the bands at 1631 and 1565 cm^{-1} observed in the DRIFT and Raman spectra, respectively, can be attributed to the asymmetric and symmetric stretching vibration modes of the C = N bond. The formation of the C = N bond is further corroborated by the peak observed at δ = 164 ppm by ^{13}C NMR (Fig. S1–S3). Furthermore, the XRD pattern (Fig. S4) and the N_2 (Fig. S5) adsorption isotherm, the latter giving a BET surface area close to 1310 m^2 g^{-1}, match those previously reported by Liu et al. [39], further confirming the successful preparation of ACOF-1. Fig. S6, S7 and S8 show the CO_2 and N_2 adsorption isotherms acquired at 273 K, 298 K and 308 K for ACOF-1, with CO_2 uptakes at 5 bar of 6.1, 4.6 and 3.9 mmol g^{-1} and N_2 uptakes of 1.2, 0.7 and 0.7 mmol g^{-1} at 273, 298 and 308 K, respectively. The obtained CO_2 uptakes at 1 bar are in good agreement with the values previously reported by Stegbauer et al. [41] ACOF-1 shows a significant preference for CO_2 adsorption over N_2, with ideal adsorption selectivities of 15, 13 and 14 based on the molar ratio of adsorbed amount of CO_2 and N_2 at 273 K, 298 K and 308 K, respectively, calculated at 1 bar. These results demonstrate that ACOF-1 is selective towards CO_2 over N_2, rendering ACOF-1 an interesting candidate for the preparation of MMMs for post-combustion CO_2 capture.

3.2. Characterization of ACOF-1-based MMMs

In order to study the influence of the polymeric matrix on membrane performance, MMMs containing ACOF-1 and 3 different polymers, namely, Matrimid®, Polyactive™ and 6FDA:DAM were prepared. Scanning electron microscopy (SEM) was used to assess the dispersion of ACOF-1 at the cross-section of the different membranes. Fig. 2a shows that ACOF-1 particles show a spherical morphology. The averaged particle size is 350 ± 30 nm calculated from transmission electron microscopy (TEM) images in our previous paper [35]. Fig. 2b-d demonstrate that ACOF-1 particles are homogeneously dispersed into the polymer matrices with no obvious interfacial voids at the filler-polymer interface. The good dispersion of the COF particles is in line with the homogenous distribution of ACOF-1 in Matrimid® previously observed by Raman spectroscopy [35].

Fig. S9 shows the thermogravimetric analyses acquired for the filler and bare polymeric membranes together with those obtained for the MMMs. The TGA of ACOF-1 shows that it is stable up to 573 K, temperature at which it starts decomposing. This temperature is higher for all three polymers, decomposing at around 740 K, 735 K and 610 K in the case of Matrimid®, 6FDA:DAM and Polyactive™, respectively. Interestingly, for all three polymers the TGA curves remain flat up to the decomposition temperature, pointing to a complete removal of the solvent in the prepared membranes upon thermal treatment. As for the MMMs, the weight-loss observed between 620 K and 680 K for the Matrimid® and 6FDA:DAM containing membranes can be attributed to the decomposition of the COF. This allowed for the evaluation of the ACOF-1 loading, which is in agreement with the nominal filler content (accuracy within 5%). This is however not the case for Polyactive™-based MMMs, for which the decomposition temperature is closer to that of the COF [35,39,42], hindering such an estimation of the COF loading.

It is well accepted that pore blockage by the polymeric chains or polymer chain rigidification at the polymer-filler interface are commonly encountered in the field of MMMs, which may lead to a decrease in the membrane gas permeability [43,44]. Hence, in this study differential scanning calorimetry (DSC) and CO_2 adsorption were performed to gain insight into these possible non-ideal interface morphologies [45]. Fig. 3 shows the CO_2 adsorption isotherms acquired for ACOF-1, pure Matrimid®, Polyactive™ and 6FDA:DAM and the MMMs containing 16 wt% COF loading. Furthermore, the estimated CO_2 uptake for the MMMs calculated as a linear combination of those uptakes for the pure components is also shown. While the calculated and experimentally obtained CO_2 uptakes coincide fairly well for Matrimid® and 6FDA:DAM-based MMMs, the experimental uptake obtained for Polyactive™-containing membranes is lower than that calculated. DSC measurements show that the T_g of the membranes is hardly affected by the presence of the COF. As shown in Table S1, only ca 2 K shift (from 594 to 596 K, from 662 to 659 K and from 222 to 221 K, for Matrimid®, 6FDA-DAM and Polyactive™ membranes, respectively) was observed for these three polymers at 16 wt% COF loading, suggesting that significant rigidification of the polymeric chains surrounding the filler particles does not take place in the prepared COF MMMs. This is in contrast to some MOF-based MMMs, for which a significant increase in T_g was observed compare to the pure polymer [46–48]. Thus, the lower uptake observed for the Polyactive-based membranes can be ascribed to the partial pore blockage of ACOF-1 pores by the more flexible polymeric chains of Polyactive™. This is in contrast to the polyimides Matrimid® and 6FDA:DAM, for which their higher glass transition temperature (T_g) endow the polymeric chains with a higher rigidity, hampering their migration into the pores. Furthermore, the lower molecular weight of Polyactive™ may also play a role, where the shorter polymeric chains might facilitate the blockage of the COF pores. A further hint into the influence of the Polyactive™ on the ACOF-1 filler particles is given by XRD. Fig. S10 shows the XRD patterns of ACOF-1, the pure polymers and the composite membranes. For ACOF-1@Matrimid® and ACOF-1@6FDA:DAM MMMs, the reflection observed at 8.3°, corresponding to the COF, indicates that the ACOF-1 crystallinity is maintained upon membrane preparation. This is not the case for Polyactive™-based membranes, for which the absence of reflections related to ACOF-1 point to the loss of long range order.

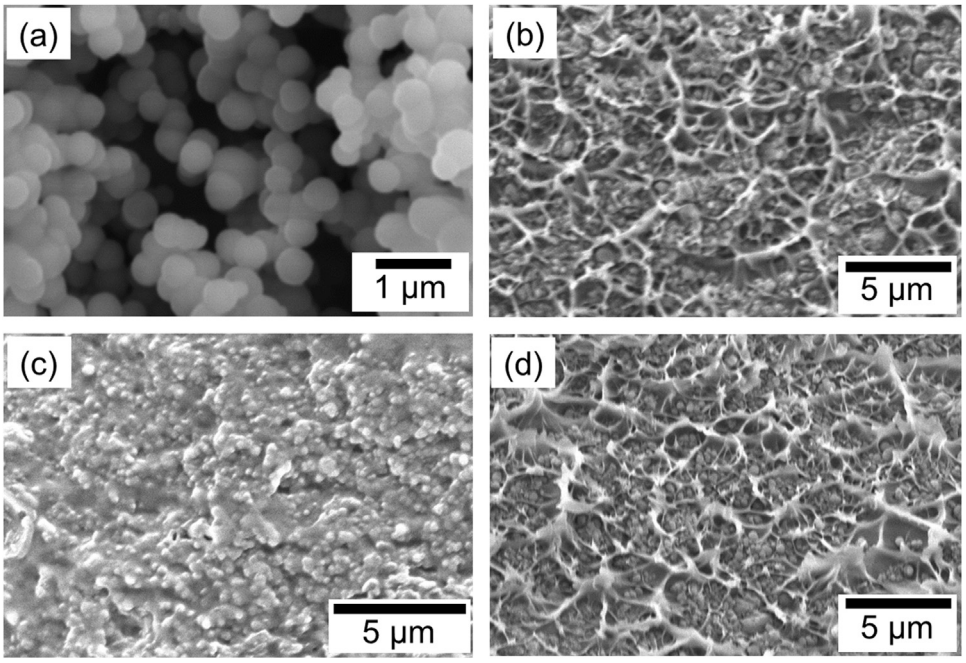

Fig. 2. SEM micrographs of (a) ACOF-1 and the cross-section of (b) 16 wt% ACOF-1@Matrimid®, (c) 16 wt% ACOF-1@Polyactive™ and (d) 16 wt% ACOF-1@6FDA:DAM MMMs.

3.3. Gas separation performance

Membranes with three different loadings (0, 8 and 16 wt%) were prepared for each polymeric matrix and tested in the separation of CO_2 from a 15:85 CO_2:N_2 gas mixture at 308 K and different feed pressures (Fig. 4 and Table S2). Each membrane was fabricated and measured at least 3 times to ensure reliable results. Fig. 4 shows the different behavior of the MMMs depending on the polymeric matrix used, pointing to the importance of a good selection of the COF/polymer pair. MMMs synthesized with Matrimid® exhibited an increase in the CO_2 and N_2 permeabilities (P_{CO2} increases from 9.5 to 17.7 Barrer upon 16 wt% COF loading) together with an increase in the CO_2/N_2 separation factor from 29 to 35. This permeability and selectivity increase, being more pronounced at higher COF loadings, is in line with our previous results, where ACOF-1@Matrimid® MMMs were studied in the separation of CO_2 from CH_4. The additional transport pathways provided by the ACOF-1 are most likely behind the improvement of the membrane permeability, while the higher selectivity can be ascribed to the preferential adsorption of CO_2 over N_2 in the N-rich ACOF-1 framework [39]. In the case of Polyactive™-based MMMs however, a pronounced permeability decrease was observed at increasing filler loadings together with a rather constant CO_2/N_2 selectivity. Pore blockage by Polyactive™ and crystallinity loss (vide supra) account for this observation. A slightly higher CO_2/N_2 selectivity is observed for the 6FDA:DAM containing MMMs with a slight decrease in CO_2 permeability for 8 wt% ACOF-1 MMMs. In this case, the absence of indications

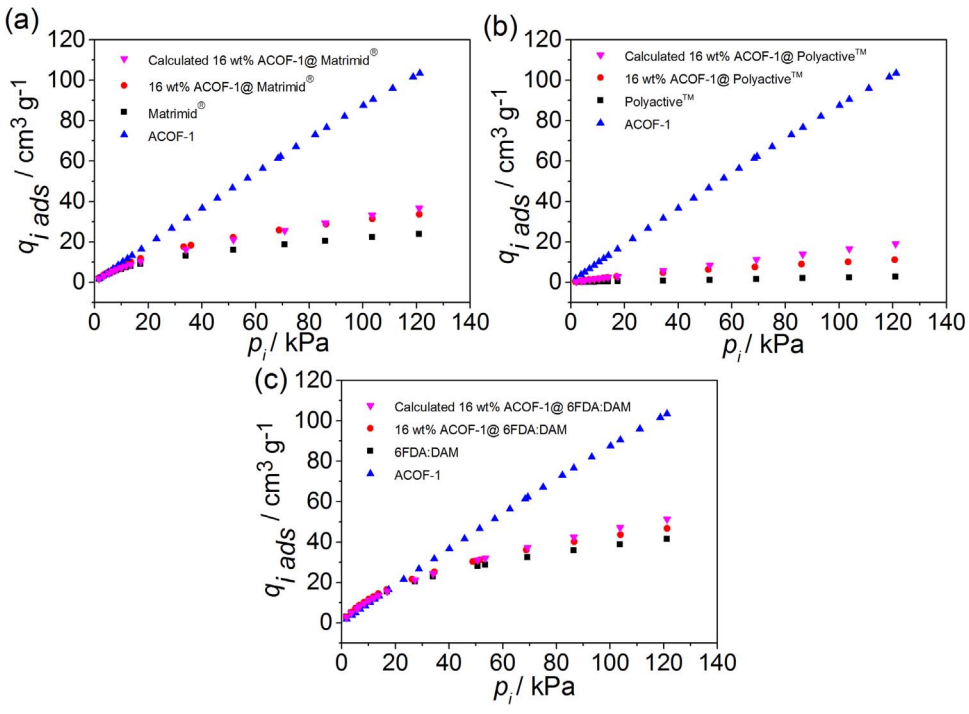

Fig. 3. CO_2 adsorption isotherms acquired at 273 K for the prepared membranes: (a) Matrimid®, (b) Polyactive™, and (c) 6 FDA:DAM.

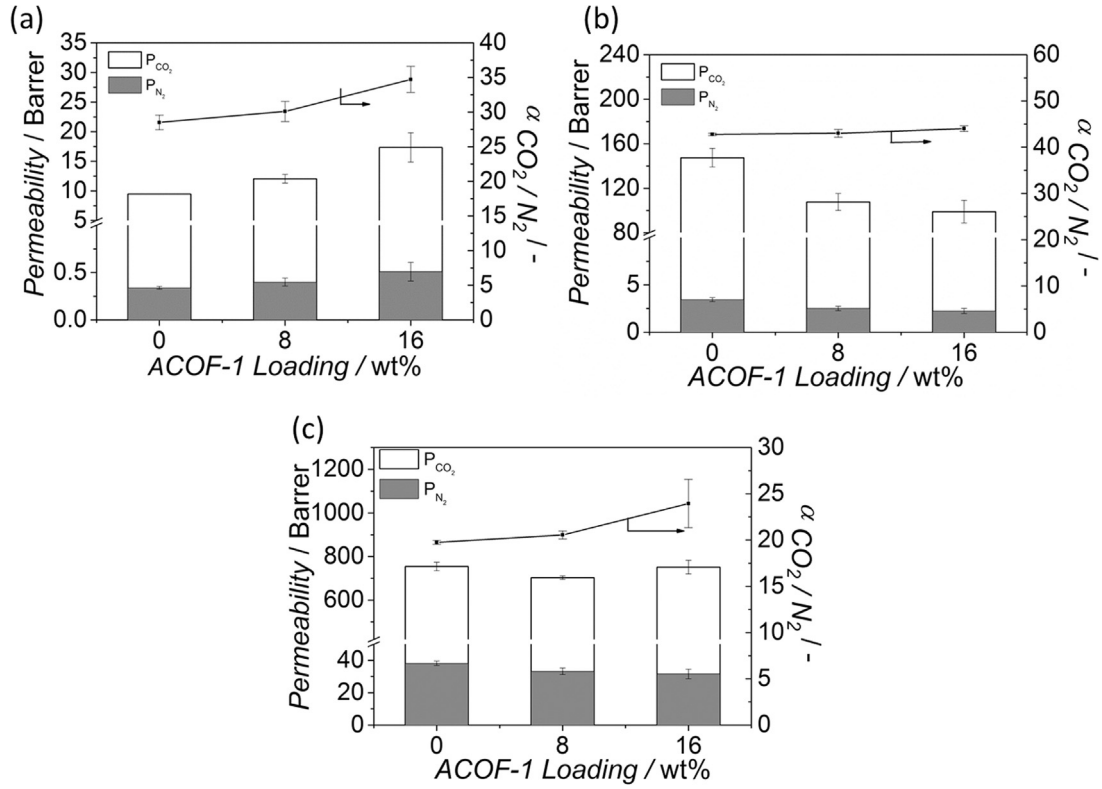

Fig. 4. Performance of MMMs based on (a) Matrimid®, (b) Polyactive™ and (c) 6FDA:DAM with different ACOF-1 loadings in the separation of CO_2 from a 15:85 CO_2/N_2 mixture at 308 K and a feed pressure of 2 bar. Error bars correspond to standard deviation.

pointing to pore blockage and reduced framework crystallinity rule out the hypothesis of a lower gas accessibility to the ACOF-1. Therefore, the observed decrease in permeability can be probably attributed to the gas permeability of ACOF-1, which is lower than the highly permeable 6FDA:DAM. This is in agreement with the calculated results reported in MOF-based MMMs, where a highly selective MOF can increase the selectivity of a highly permeable polymer but slightly decreases the MMM's CO_2 permeability [37]. At higher COF loadings (16 wt% and 24 wt%) however the membrane permeability increases together with a constant or decreased selectivity for 16 and 24 wt% COF loading, respectively. This points to the formation of defects at the COF/polymer interface when the filler content is further increased.

The influence of feed pressure on the gas permeation performance of neat polymers and MMMs is shown in Fig. 5. The permeability of Matrimid® and 6FDA:DAM containing membranes shows a slight decrease with increasing feed pressure, what is attributed to the saturation of Langmuir adsorption sites following the well-known dual-mode sorption model [49]. Similar results have been reported for other MOF-based MMMs [44,50]. For the case of rubbery Polyactive™, the gas solubility obeys Henry's law, where the solubility for each gas through the membrane is directly proportional to the applied pressure [51]. Therefore, the gas permeability of Polyactive™ membranes remained relatively constant over the whole pressure test range.

The results for the three neat polymers and the MMMs were put into perspective using the 2008 Robeson plot. Fig. 6 shows the CO_2 permeabilities together with CO_2/N_2 selectivities for neat polymer membranes and the MMMs measured at 308 K and a feed pressure of 2 bar together with some relevant results for CO_2/N_2 separation reported for MOF-based MMMs [21]. The results of the three bare polymer membranes from this work are in line with the previous literature. Although none of our results surpass the Robeson upper bound, the incorporation of ACOF-1 results in a clear improvement in the membranes containing Matrimid® and 6FDA:DAM. Specifically, the best results were observed for MMMs based on Matrimid®, which showed an enhancement in both CO_2 permeability and CO_2/N_2 selectivity upon ACOF-1 loading. To gain further insight into the behavior of these best-performing membranes, one of the 16 wt% ACOF-1@Matrimid® MMMs was re-tested after one year (Table S3). Results show that the separation performance is maintained, pointing to a good stability of the prepared membranes. In contrast to Matrimid®-based MMM, 6FDA:DAM and Polyactive™-containing MMMs exhibit a decrease in membrane permeability, which only in the case of 6FDA:DAM takes place together with an increase in membrane selectivity.

4. Conclusions

MMMs comprising ACOF-1 were prepared with 2 different filler loadings and 3 different polymer matrices. Among the different polymers chosen, the best results were obtained for Matrimid®, for which non-idealities were not observed at the filler-polymer interface and whose low permeability allows for an improvement in membrane permeability upon filler dispersion. In the case of Polyactive™ and 6FDA:DAM however, a decrease in membrane permeability was observed. In the former case, pore blockage by the more flexible polymeric chains together with a loss in long range order of the filler accounts for the poorer membrane performance. In the latter case, the additional transport pathways provided by the COF are not sufficient to improve the permeability of the already highly permeable polymeric matrix, the composite membranes showing a higher selectivity in line with the still accessible filler pores.

Overall, our results demonstrate that the combination of the filler-polymeric matrix pair chosen is crucial, and should be helpful for the application of COFs in the next-generation hybrid membrane fields. For a given filler the polymer performance improvement strongly depends on the polymeric matrix selected, where a good match between the discontinuous and continuous phase, both in the terms of compatibility and gas separation properties, is necessary to optimize membrane performance.

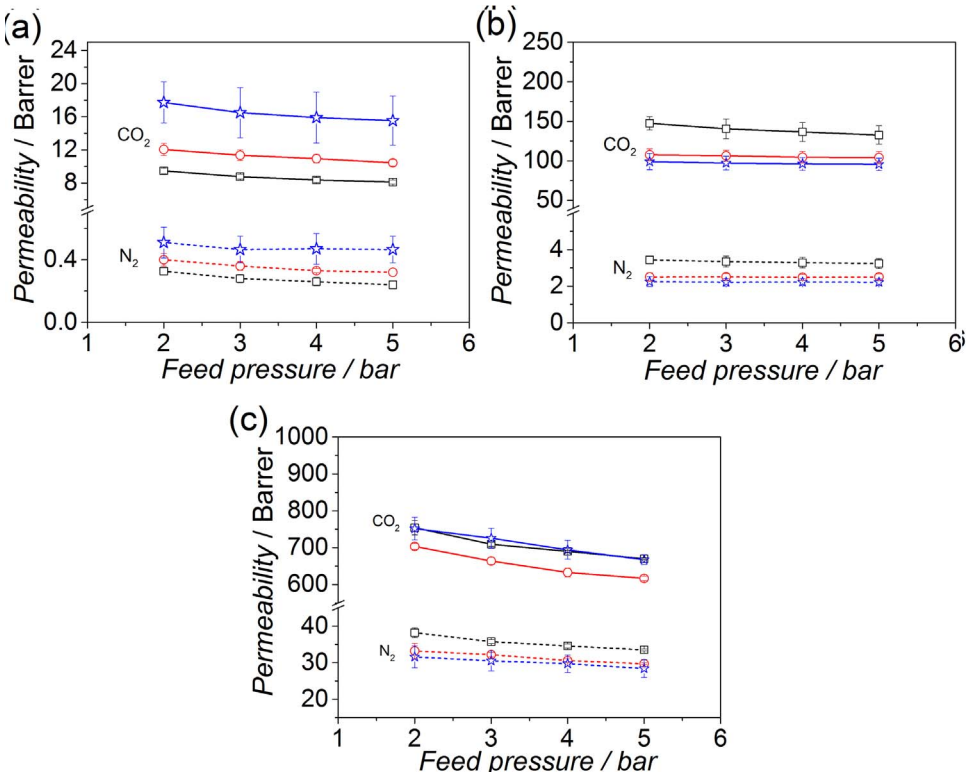

Fig. 5. Effect of the feed pressure on the gas separation performance of (a) Matrimid®, (b) Polyactive™ and (c) 6FDA:DAM containing membranes. Results obtained in the separation of CO_2 from a 15:85 CO_2/N_2 mixture at 308 K. Error bars correspond to standard deviation. □ Pure polymer, ○ 8 wt% ACOF-1 MMMs, ☆ 16 wt% ACOF-1 MMMs.

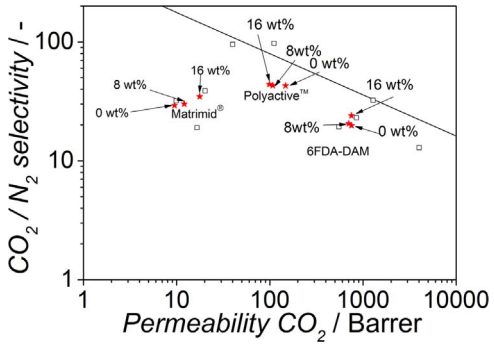

Fig. 6. Robeson plot for the separation of CO_2 from a 15:85 CO_2/N_2 mixture at 308 K and a feed pressure of 2 bar, showing the gas separation performance of three pure polymers used in this study together with their MMMs (with 8 and 16 wt% ACOF loading). Most relevant results [13,52–59] reported in the literature for MOF-based MMMs have also been included for comparison (open squares). See detailed information in Table S4.

Acknowledgements

B.S. gratefully acknowledges the Netherlands National Science Foundation 722.015.007 (NWO) for her personal VENI grant. J.G. acknowledges financial support of the European Research Council under the European Union's Seventh Framework Programme, ERC Grant Agreement no. 335746, CrystEng-MOF-MMM. Meixia Shan gratefully acknowledges the support from the China Scholarship Council.

Appendix A. Supplementary material

Supplementary data associated with this article can be found in the online version at http://dx.doi.org/10.1016/j.memsci.2017.12.008.

References

[1] R.T. Woodward, L.A. Stevens, R. Dawson, M. Vijayaraghavan, T. Hasell, I.P. Silverwood, A.V. Ewing, T. Ratvijitvech, J.D. Exley, S.Y. Chong, F. Blanc, D.J. Adams, S.G. Kazarian, C.E. Snape, T.C. Drage, A.I. Cooper, Swellable, water- and acid-tolerant polymer sponges for chemoselective carbon dioxide capture, J. Am. Chem. Soc. 136 (2014) 9028–9035.

[2] M.S. Lee, M. Park, H.Y. Kim, S.J. Park, Effects of microporosity and surface chemistry on separation performances of n-containing pitch-based activated carbons for CO_2/N_2 binary mixture, Sci. Rep. 6 (2016) 23224.

[3] J. Wang, Q. Liu, An efficient one-step condensation and activation strategy to synthesize porous carbons with optimal micropore sizes for highly selective CO_2 adsorption, Nanoscale 6 (2014) 4148–4156.

[4] P. Arab, E. Parrish, T. Islamoglu, H.M. El-Kaderi, Synthesis and evaluation of porous azo-linked polymers for carbon dioxide capture and separation, J. Mater. Chem. A (2015) 20586–20594.

[5] H.A. Patel, S. Hyun Je, J. Park, D.P. Chen, Y. Jung, C.T. Yavuz, A. Coskun, Unprecedented high-temperature CO_2 selectivity in N_2-phobic nanoporous covalent organic polymers, Nat. Commun. 4 (2013) 1357.

[6] M. Shan, Q. Xue, N. Jing, C. Ling, T. Zhang, Z. Yan, J. Zheng, Influence of chemical functionalization on the CO_2/N_2 separation performance of porous graphene membranes, Nanoscale 4 (2012) 5477–5482.

[7] L.M. Robeson, Correlation of separation factor versus permeability for polymeric membranes, J. Membr. Sci. 62 (1991) 165–185.

[8] L.M. Robeson, The upper bound revisited, J. Membr. Sci. 320 (2008) 390–400.

[9] A. Bos, I.G.M. Pünt, M. Wessling, H. Strathmann, CO_2-induced plasticization phenomena in glassy polymers, J. Membr. Sci. 155 (1999) 67–78.

[10] R. Swaidan, B. Ghanem, E. Litwiller, I. Pinnau, Physical aging, plasticization and their effects on gas permeation in "rigid" polymers of intrinsic microporosity, Macromolecules 48 (2015) 6553–6561.

[11] X. Wang, C. Chi, K. Zhang, Y. Qian, K.M. Gupta, Z. Kang, J. Jiang, D. Zhao, Reversed thermo-switchable molecular sieving membranes composed of two-dimensional metal-organic nanosheets for gas separation, Nat. Commun. 8 (2017) 14460.

[12] J.E. Bachman, J.R. Long, Plasticization-resistant Ni_2(dobdc)/polyimide composite membranes for the removal of CO_2 from natural gas, Energy Environ. Sci. 9 (2016) 2031–2036.

[13] Q. Song, S.K. Nataraj, M.V. Roussenova, J.C. Tan, D.J. Hughes, W. Li, P. Bourgoin, M.A. Alam, A.K. Cheetham, S.A. Al-Muhtaseb, E. Sivaniah, Zeolitic imidazolate framework (ZIF-8) based polymer nanocomposite membranes for gas separation, Energy Environ. Sci. 5 (2012) 8359–8369.

[14] B. Zornoza, A. Martinez-Joaristi, P. Serra-Crespo, C. Tellez, J. Coronas, J. Gascon, F. Kapteijn, Functionalized flexible MOFs as fillers in mixed matrix membranes for highly selective separation of CO_2 from CH_4 at elevated pressures, Chem. Commun. 47 (2011) 9522–9524.

[15] J. Sánchez-Laínez, B. Zornoza, S. Friebe, J. Caro, S. Cao, A. Sabetghadam, B. Seoane, J. Gascon, F. Kapteijn, C. Le Guillouzer, G. Clet, M. Daturi, C. Téllez, J. Coronas, Influence of ZIF-8 particle size in the performance of polybenzimidazole mixed matrix membranes for pre-combustion CO_2 capture and its validation through interlaboratory test, J. Membr. Sci. 515 (2016) 45–53.

[16] J. Sanchez-Lainez, B. Zornoza, C. Tellez, J. Coronas, On the chemical filler-polymer interaction of nano- and micro-sized ZIF-11 in PBI mixed matrix membranes and

their application for H_2/CO_2 separation, J. Mater. Chem. A 4 (2016) 14334–14341.
[17] I. Kiesow, D. Marczewski, L. Reinhardt, M. Mühlmann, M. Possiwan, W.A. Goedel, Bicontinuous zeolite polymer composite membranes prepared via float casting, J. Am. Chem. Soc. 135 (2013) 4380–4388.
[18] T.S. Chung, S.S. Chan, R. Wang, Z. Lu, C. He, Characterization of permeability and sorption in Matrimid/C60 mixed matrix membranes, J. Membr. Sci. 211 (2003) 91–99.
[19] T. Rodenas, M. van Dalen, E. García-Pérez, P. Serra-Crespo, B. Zornoza, F. Kapteijn, J. Gascon, Visualizing MOF mixed matrix membranes at the nanoscale: towards structure-performance relationships in CO_2/CH_4 separation over NH_2-MIL-53(Al)@PI, Adv. Funct. Mater. 24 (2014) 249–256.
[20] X. Liu, H. Jin, Y. Li, H. Bux, Z. Hu, Y. Ban, W. Yang, Metal–organic framework ZIF-8 nanocomposite membrane for efficient recovery of furfural via pervaporation and vapor permeation, J. Membr. Sci. 428 (2013) 498–506.
[21] B. Seoane, J. Coronas, I. Gascon, M.E. Benavides, O. Karvan, J. Caro, F. Kapteijn, J. Gascon, Metal-organic framework based mixed matrix membranes: a solution for highly efficient CO_2 capture? Chem. Soc. Rev. 44 (2015) 2421–2454.
[22] N.C. Burtch, H. Jasuja, K.S. Walton, Water stability and adsorption in metal–organic frameworks, Chem. Rev. 114 (2014) 10575–10612.
[23] X. Feng, X. Ding, D. Jiang, Covalent organic frameworks, Chem. Soc. Rev. 41 (2012) 6010–6022.
[24] J.L. Mendoza-Cortes, W.A. Goddard, H. Furukawa, O.M. Yaghi, A covalent organic framework that exceeds the doe 2015 volumetric target for H_2 uptake at 298 K, J. Phys. Chem. Lett. 3 (2012) 2671–2675.
[25] M.G. Rabbani, A.K. Sekizkardes, Z. Kahveci, T.E. Reich, R. Ding, H.M. El-Kaderi, A 2D mesoporous imine-linked covalent organic framework for high pressure gas storage applications, Chem. Eur. J. 19 (2013) 3324–3328.
[26] C.E. Chan-Thaw, A. Villa, P. Katekomol, D. Su, A. Thomas, L. Prati, Covalent triazine framework as catalytic support for liquid phase reaction, Nano Lett. 10 (2010) 537–541.
[27] S. Jin, X. Ding, X. Feng, M. Supur, K. Furukawa, S. Takahashi, M. Addicoat, M.E. El-Khouly, T. Nakamura, S. Irle, S. Fukuzumi, A. Nagai, D. Jiang, Charge dynamics in a donor–acceptor covalent organic framework with periodically ordered bicontinuous heterojunctions, Angew. Chem. Int. Ed. 52 (2013) 2017–2021.
[28] X. Wu, Z. Tian, S. Wang, D. Peng, L. Yang, Y. Wu, Q. Xin, H. Wu, Z. Jiang, Mixed matrix membranes comprising polymers of intrinsic microporosity and covalent organic framework for gas separation, J. Membr. Sci. 528 (2017) 273–283.
[29] L. Xu, J. Xu, B. Shan, X. Wang, C. Gao, TpPa-2-incorporated mixed matrix membranes for efficient water purification, J. Membr. Sci. 526 (2017) 355–366.
[30] J. Dechnik, J. Gascon, C. Doonan, C. Janiak, C.J. Sumby, Mixed-matrix membranes, Angew. Chem., Int. Ed. 32 (2017) 9292–9310.
[31] G. Yu, H. Rong, X. Zou, G. Zhu, Engineering microporous organic framework membranes for CO_2 separations, Mol. Syst. Des. Eng. 2 (2017) 182–190.
[32] U.K. Kharul, R. Banerjee, B. Biswal, H.D. Chaudhari, Chemically stable covalent organic framework (COF)-polybenzimidazole hybrid membranes: enhanced gas separation through pore modulation, Chem. Eur. J. 22 (2016) 4695–4699.
[33] X. Cao, Z. Qiao, Z. Wang, S. Zhao, P. Li, J. Wang, S. Wang, Enhanced performance of mixed matrix membrane by incorporating a highly compatible covalent organic framework into poly(vinylamine) for hydrogen purification, Int. J. Hydrog. Energy 21 (2016) 9167–9174.
[34] Z. Kang, Y. Peng, Y. Qian, D. Yuan, M.A. Addicoat, T. Heine, Z. Hu, L. Tee, Z. Guo, D. Zhao, Mixed matrix membranes (MMMs) comprising exfoliated 2D covalent organic frameworks (COFs) for efficient CO_2 separation, Chem. Mater. 28 (2016) 1277–1285.
[35] M. Shan, B. Seoane, E. Rozhko, A. Dikhtiarenko, G. Clet, F. Kapteijn, J. Gascon, Azine-linked covalent organic framework (COF)-based mixed-matrix membranes for CO_2/CH_4 Separation, Chem. Eur. J. 22 (2016) 14467–14470.
[36] T.H. Bae, J.S. Lee, W. Qiu, W.J. Koros, C.W. Jones, S. Nair, A high-performance gas-separation membrane containing submicrometer-sized metal–organic framework crystals, Angew. Chem. Int. Ed. 49 (2010) 9863–9866.
[37] S. Keskin, D.S. Sholl, Selecting metal organic frameworks as enabling materials in mixed matrix membranes for high efficiency natural gas purification, Energy Environ. Sci. 3 (2010) 343–351.
[38] G. Yilmaz, S. Keskin, Molecular modeling of MOF and ZIF-filled MMMs for CO_2/N_2 separations, J. Membr. Sci. 454 (2014) 407–417.
[39] Z. Li, X. Feng, Y. Zou, Y. Zhang, H. Xia, X. Liu, Y. Mu, A 2D azine-linked covalent organic framework for gas storage applications, Chem. Commun. 50 (2014) 13825–13828.
[40] P. Badrinarayanan, W. Zheng, Q. Li, S.L. Simon, The glass transition temperature versus the fictive temperature, J. Non-Cryst. Solids 353 (2007) 2603–2612.
[41] L. Stegbauer, M.W. Hahn, A. Jentys, G. Savasci, C. Ochsenfeld, J.A. Lercher, B.V. Lotsch, Tunable water and CO_2 sorption properties in isostructural azine-based covalent organic frameworks through polarity engineering, Chem. Mater. 27 (2015) 7874–7881.
[42] A. Car, C. Stropnik, W. Yave, K.V. Peinemann, Tailor-made polymeric membranes based on segmented block copolymers for CO_2 separation, Adv. Funct. Mater. 18 (2008) 2815–2823.
[43] Y. Li, T.S. Chung, C. Cao, S. Kulprathipanja, The effects of polymer chain rigidification, zeolite pore size and pore blockage on polyethersulfone (PES)-zeolite A mixed matrix membranes, J. Membr. Sci. 260 (2005) 45–55.
[44] A. Sabetghadam, B. Seoane, D. Keskin, N. Duim, T. Rodenas, S. Shahid, S. Sorribas, C.L. Guillouzer, G. Clet, C. Tellez, Metal organic framework crystals in mixed-matrix membranes: impact of the filler morphology on the gas separation performance, Adv. Funct. Mater. 18 (2016) 3154–3163.
[45] T.S. Chung, L.Y. Jiang, Y. Li, S. Kulprathipanja, Mixed matrix membranes (MMMs) comprising organic polymers with dispersed inorganic fillers for gas separation, Prog. Polym. Sci. 32 (2007) 483–507.
[46] A.L. Khan, C. Klaysom, A. Gahlaut, X. Li, I.F.J. Vankelecom, SPEEK and functionalized mesoporous MCM-41 mixed matrix membranes for CO_2 separations, J. Mater. Chem. 22 (2012) 20057–20064.
[47] M.W. Anjum, F. Vermoortele, A.L. Khan, B. Bueken, D.E. De Vos, I.F.J. Vankelecom, Modulated UiO-66-based mixed-matrix membranes for CO_2 separation, ACS Appl. Mater. Interfaces 7 (2015) 25193–25201.
[48] N. Tien-Binh, H. Vinh-Thang, X.Y. Chen, D. Rodrigue, S. Kaliaguine, Polymer functionalization to enhance interface quality of mixed matrix membranes for high CO_2/CH_4 gas separation, J. Mater. Chem. A 3 (2015) 15202–15213.
[49] S. Kanehashi, K. Nagai, Analysis of dual-mode model parameters for gas sorption in glassy polymers, J. Membr. Sci. 253 (2005) 117–138.
[50] S. Shahid, K. Nijmeijer, Performance and plasticization behavior of polymer–MOF membranes for gas separation at elevated pressures, J. Membr. Sci. 470 (2014) 166–177.
[51] V. Stannett, The transport of gases in synthetic polymeric membranes – an historic perspective, J. Membr. Sci. 3 (1978) 97–115.
[52] Y. Zhang, I.H. Musselman, J.P. Ferraris, K.J. Balkus, Gas permeability properties of Matrimid® membranes containing the metal-organic framework Cu–BPY–HFS, J. Membr. Sci. 313 (2008) 170–181.
[53] E.V. Perez, K.J. Balkus, J.P. Ferraris, I.H. Musselman, Mixed-matrix membranes containing MOF-5 for gas separations, J. Membr. Sci. 328 (2009) 165–173.
[54] J.O. Hsieh, K.J. Balkus, J.P. Ferraris, I.H. Musselman, MIL-53 frameworks in mixed-matrix membranes, Microporous Mesoporous Mater. 196 (2014) 165–174.
[55] T. Li, Y. Pan, K.V. Peinemann, Z. Lai, Carbon dioxide selective mixed matrix composite membrane containing ZIF-7 nano-fillers, J. Membr. Sci. 425 (2013) 235–242.
[56] R.P. Lively, M.E. Dose, L. Xu, J.T. Vaughn, J.R. Johnson, J.A. Thompson, K. Zhang, M.E. Lydon, J.-S. Lee, L. Liu, Z. Hu, O. Karvan, M.J. Realff, W.J. Koros, A high-flux polyimide hollow fiber membrane to minimize footprint and energy penalty for CO_2 recovery from flue gas, J. Membr. Sci. 423 (2012) 302–313.
[57] T.H. Bae, J.R. Long, CO_2/N_2 separations with mixed-matrix membranes containing Mg_2(dobdc) nanocrystals, Energy Environ. Sci. 6 (2013) 3565–3569.
[58] V. Nafisi, M.B. Hägg, Development of dual layer of ZIF-8/PEBAX-2533 mixed matrix membrane for CO_2 capture, J. Membr. Sci. 459 (2014) 244–255.
[59] S. Japip, H. Wang, Y. Xiao, T. Shung Chung, Highly permeable zeolitic imidazolate framework (ZIF)-71 nano-particles enhanced polyimide membranes for gas separation, J. Membr. Sci. 467 (2014) 162–174.